

Article

Research on the Performance of Regenerant Modified Cold Recycled Mixture with Asphalt Emulsions

Decai Wang ¹, Tengteng Guo ^{1,*}, Haolei Chang ², Xianhua Yao ¹ , Yuanzhao Chen ¹  and Tongning Wang ¹

¹ School of Civil Engineering and Communication, North China University of Water Resources and Electric Power, Zhengzhou 450045, China; wangdecai@ncwu.edu.cn (D.W.); yaoxianhua@ncwu.edu.cn (X.Y.); cyz740513@ncwu.edu.cn (Y.C.); wangtongning@ncwu.edu.cn (T.W.)

² School of Water Conservancy and Environment, Zhengzhou University, Zhengzhou 450001, China; changhaolei@gs.zzu.edu.cn

* Correspondence: guotth@ncwu.edu.cn

Abstract: In order to study the mechanical properties and effect of a regenerant on a cold recycled mixture with asphalt emulsions (CRMEs), the moisture susceptibility, high-temperature performance, low-temperature performance, dynamic mechanical properties and durability of CRMEs were analyzed and evaluated by immersion splitting strength tests, freeze-thaw splitting strength tests, rutting tests, semi-circle bending tests, uniaxial compression dynamic modulus tests and indirect tensile tests. Scanning electron microscopy (SEM) was used to analyze the micromorphology of CRMEs modified with regenerant. Finally, a comprehensive evaluation system of five different CRMEs was established based on the efficacy coefficient method to quantitatively analyze the comprehensive performance of the CRMEs. The test results showed that the regenerant can significantly improve the water immersion splitting strength, freeze-thaw splitting strength fracture energy density, and fatigue resistance of CRMEs. However, the addition of regenerant affected the high-temperature performance of the cold recycled mixture. The dynamic modulus of the CRMEs first increased and then decreased with regenerant content increasing. When the regenerant content was 8%, the dynamic modulus of the CRMEs was the highest. Adding styrene-butadiene rubber (SBR) latex can improve the high-temperature performance of CRMEs, but the moisture susceptibility, low temperature performance and fatigue resistance of the cold recycled mixture were not significantly improved, and the dynamic modulus of the mixture was reduced. Based on the efficacy coefficient method, the optimal content of regenerant is 8%. Regenerant are potential modifiers for cold recycled mixture that they can significantly improve the dynamic mechanical properties and durability.

Keywords: cold recycled mixture; emulsified asphalt; regenerant; performance; efficacy coefficient method



Citation: Wang, D.; Guo, T.; Chang, H.; Yao, X.; Chen, Y.; Wang, T. Research on the Performance of Regenerant Modified Cold Recycled Mixture with Asphalt Emulsions. *Sustainability* **2021**, *13*, 7284. <https://doi.org/10.3390/su13137284>

Received: 11 May 2021
Accepted: 19 June 2021
Published: 29 June 2021

Publisher's Note: MDPI stays neutral with regard to jurisdictional claims in published maps and institutional affiliations.



Copyright: © 2021 by the authors. Licensee MDPI, Basel, Switzerland. This article is an open access article distributed under the terms and conditions of the Creative Commons Attribution (CC BY) license (<https://creativecommons.org/licenses/by/4.0/>).

1. Introduction

Emulsified asphalt cold recycling technology is a green road construction method with broad application prospects that has the advantages of energy savings, environmental protection, and low cost. It is widely used in asphalt pavement renovation and reconstruction projects [1,2]. With the role of the application of this technology in asphalt pavement structure growing (such as with use in the middle course of highways) [3–5], higher technical requirements are also being put forward for the performance of cold recycled mixture with asphalt emulsions (CRMEs). Therefore, improving the performance of CRMEs and the application level of the CRME structure layer has become an important problem to be solved by engineers.

In view of the shortcomings of emulsified asphalt cold recycling methods (such as insufficient mechanical performance and poor durability), scholars in various countries have carried out work on improving the performance of cold recycled mixtures. Daryae evaluated the fatigue resistance, moisture susceptibility and rutting resistance of the CRMEs

through a four-point trabecular fatigue test, indirect tensile strength test and dynamic creep test. The results show that the use of regenerant (RE), waste polymer and emulsified asphalt at the same time in 50% reclaimed asphalt pavement (RAP) mixture can significantly enhance the fatigue resistance, rutting resistance and moisture susceptibility of the CRME [6]. Ali conducted indirect tensile strength test, elastic modulus test, moisture susceptibility test, and dynamic creep test on CRME added with Portland cement, fly ash, and rice husk ash. The test results show that Portland cement is the best effective additives, while the mechanical properties of CRME with fly ash and rice husk ash are not improved much [7]. Ayar found that cement can improve the short-term and long-term performance of recycled mixture with bitumen emulsion owing to its interaction with asphalt. Slurry lime could superiorly improve the durability of the recycled mixture with bitumen emulsion compared with lime powder [8]. Wang found that acrylic copolymer emulsion can significantly reduce the air void content and improve the moisture damage resistance of the cold recycled mixtures [9]. Mohsen performed Marshall stability tests, indirect tensile strength tests, and moisture susceptibility tests on CRMEs of different ages with added cement kiln dust (CKD) and cinder ash (CA). They found that the combined use of CKD and CA can significantly improve the mechanical properties of the cold recycled mixture [10]. J Jiang prepared three different kinds of latex modified emulsified asphalt cold recycled mixture and researched the rutting resistance of full-depth pavement structures of cold recycled mixtures by high temperature dynamic shear rheology tests and multiple stress creep recovery tests. The test results showed that neoprene latex can significantly enhance the high-temperature performance of cold recycled mixture pavement [11]. Dongguang Yang investigated the influence of different kinds and contents of fiber on the pavement performance and durability of CRMEs by a four-point bending fatigue test [12]. Deng studied the influence of mineral filler, machine-made sand, coarse aggregate and other virgin aggregate contents on the performance of emulsified asphalt cold recycled mixture prepared by the vertical vibration compaction method. The research results suggest that the optimal content of mineral filler, machine-made sand and coarse aggregate is 3%, 20% and 10–30%, respectively [13]. Qingkui Han researched the effect of styrene-butadiene rubber (SBR) latex on the low-temperature performance of CRMEs, and found that SBR latex can significantly improve the flexural stiffness modulus and flexural strength of the CRMEs [14]. Yafei Li studied the effects of the waterborne epoxy resin on the early strength and durability of CRMEs. The test results showed that waterborne epoxy resin can significantly improve the early strength, high-temperature and low-temperature performance and durability of the mixture [15]. Cheng Chen carried out laboratory tests and found that rubber powder can markedly improve the early strength, low temperature crack resistance and fatigue performance of cold recycled mixture [16].

In addition, some scholars have also carried out related research on factors that influence the performance of CRMEs and obtained the following results: Junxiao Li studied the effect of the cement and RAP ratio on the moisture susceptibility of cold recycled mixture. The test results showed that an appropriate content of cement can improve the moisture susceptibility of CRMEs. The higher the RAP content is, the lower the moisture susceptibility of the mixture [17]. Jinhai Yan used a Cooper testing machine to test the indirect tensile fatigue performance of CRMEs at 15 °C and the stiffness modulus at different temperatures and stress levels [18]. Stimuli evaluated and analyzed the properties of CRMEs with a high content of old asphalt materials that were used in the lower layer of an expressway. The volume parameters, stiffness, permanent deformation and fatigue properties of the mixture were studied through the testing of road core samples and indoor specimens [19]. Lyu analyzed the influence of each component content in CRMEs on its comprehensive performance based on the weighted grey target theory. The results show that the content of emulsified asphalt and cement mainly affects the high-temperature performance of cold recycled mixture, while the content of RAP has a greater impact on the moisture susceptibility, and both of the factors can significantly affect the fatigue performance [20]. Zhang comprehensively analyzed the effects of 10 factors on the low-

temperature crack resistance of cold recycled mixture using semicircular bending tests and found that the addition of regenerant improved the low-temperature crack resistance of mixture accounts by more than 60% [21]. Yuhui Pi studied the strength formation mechanism of CRMEs through microscopic tests and analyzed the influence of aggregate gradation, emulsified asphalt content, water content, and cement content on their strength through laboratory tests. It was finally determined that the optimal contents of emulsified asphalt and cement in the recycled mixture are 2.9% and 1.5%, respectively [22]. Zhigang Li measured the void ratio, penetration shear strength and unconfined compressive strength after different freeze-thaw cycles to determine the decay law of the mechanical properties and shear strength parameters of the CRMEs [23].

In recent years, some studies have also involved the microscopic morphology analysis of CRMEs. Tangzhong Wei analyzed the hydration reaction and emulsified asphalt demulsification process in cement emulsified asphalt mortar with the help of scanning electron microscopy (SEM) and other microdetection methods, and found that cement can promote a rapid increase in the early strength of the CRMEs [24]. Based on the analysis of gel chromatography, infrared spectroscopy and contact angle testing methods, Liang Liu found that after RAP was treated with trichloroethylene and a silane coupling agent-modified $\text{Ca}(\text{OH})_2$ slurry, the performance of the prepared mixture was significantly improved [25]. Zhigang Li used scanning electron microscopy to observe the surface microscopy morphology of the CRMEs and quantitatively analyzed the cement hydration products by a nanometer-scale measuring instrument. The test results showed that the filler content can remarkably affect the number of fibers produced by cement hydration which have an important role in anchoring reinforcement and crack resistance of CRMEs [26]. Yanhai Yang carried out scanning electron microscopy observations and electronic energy spectrum analysis of CRMEs with cement. The results showed that cement can react with the water phase of the mixture to form fibrous crystals, which can effectively improve the early strength of the mixture [27].

In summary, the current research on CRMEs mainly focuses on the effects of Portland cement, lime, epoxy resin, chemical fiber and other modification methods, as well as the influence of factors such as curing temperature and material composition on the mechanical properties, high-temperature performance and low-temperature performance, moisture susceptibility and fatigue performance of CRMEs. Micro-experimental studies on CRMEs have mostly focused on the mechanism of the effect of cement content on the performance of cold recycled mixture, while studies on the performance and micromechanism of CRMEs modified by regenerant are fewer. Therefore, this research conducts laboratory experiments and SEM observation on the performance of CRMEs with different contents of regenerant to analysis of their modification mechanism and evaluation of the effect of modification to further improve the performance of the CRMEs and extend the service life of the recycled pavement.

2. Materials and Methods

2.1. Materials

2.1.1. Reclaimed Asphalt Pavement (RAP)

RAP material was obtained from surface milling materials of a highway. It had a moisture content of 0.42% and a recycled asphalt content of 4.87%. The result of the penetration test at 25 °C was 24.1 mm, the softening point was 60.8 °C, the ductility at 15 °C was 11.6 cm, and the viscosity at 60 °C was 2831 Pa s. The gradation composition are shown in Table 1.

Table 1. Gradation composition before and after reclaimed asphalt pavement (RAP) extraction.

Sieve pore diameter/mm	26.5	19	16	13.2	9.5	4.75	2.36	1.18	0.6	0.3	0.15	0.075
Before extracting/%	97.4	90.5	86.7	80.5	69.8	39.7	24.4	14.0	8.0	3.7	2.1	1.1
After extracting/%	100	100	98.2	93.0	83.7	61.3	43.9	36.6	29.4	18.8	14.1	10.9

2.1.2. Emulsified Asphalt

The virgin asphalt used in this study was No. 70 petroleum asphalt [28]. Emulsifiers commonly used in engineering for cold regeneration were chosen, and the water was city drinking tap water. The emulsified asphalt was prepared by colloid mill. Its residue on the sieve (1.18 mm sieve) index was 0.05, the residual content was 63.1%, the penetration rate was 76/0.1 mm at 25 °C, the ductility was 58.6 cm at 15 °C, and the Engela viscosity (E25) was 6.1. The storage stability at room temperature was 0.4% for 1 day and 1.3% for 5 days.

2.1.3. Regenerant and Styrene-Butadiene Rubber (SBR) Latex

The viscosity of the regenerant used in this research was 2.3 Pa·s at 60 °C with a 25% saturated content and a 75% aromatic content. The mass change before and after Rotating Thin-film Oven Test (RTFOT) of the regenerant was 1.6%, and the viscosity ratio was 2.1. This kind of regenerant that has high viscosity at room temperature was dissolved in a volatile organic solvent at a ratio of 1:2 and sprayed on the surface of the RAP evenly. The SBR latex used in this research had the cationic charge, a solid content of 50%, pH 5~7, and mechanical stability (5 min) of $\leq 1\%$.

2.1.4. Materials Composition Design

According to the gradation design requirements of CRMEs in JTG/T 5521 [29], 10% limestone macadam of 10~20 mm was added, and the composite gradation composition is shown in Figure 1. The cement used in this research was ordinary Portland cement with a strength grade of 32.5 and water content of 1.5%.

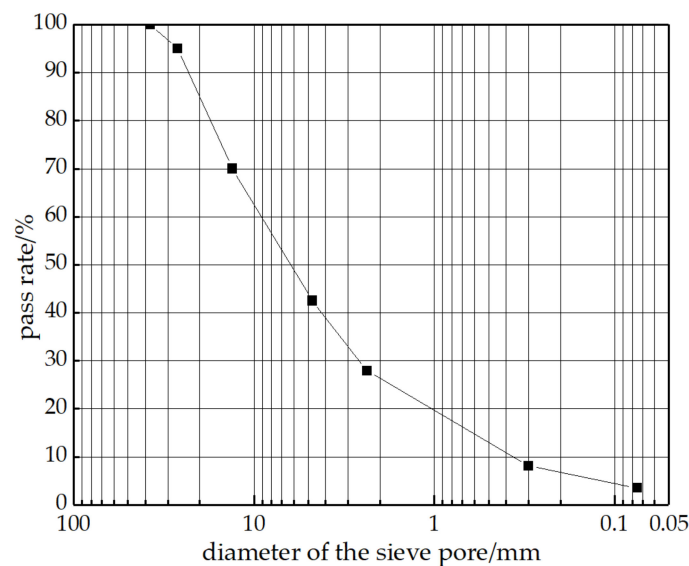


Figure 1. Gradation of emulsified asphalt cold recycled mixture.

2.2. Testing Methods

2.2.1. Testing Parameters

The specimens (diameter 101.6 mm, height 63.5 mm) were formed by a compaction method involving 50 rotations. The optimal emulsified asphalt dose and mixing water consumption were determined based on the maximum splitting strength and dry density of the specimen, and were 4.0% and 3.6%, respectively. The curing conditions of the specimens were as follows: First, the specimen was cured for 24 h at room temperature and then put into a 40 °C blast oven for accelerated curing for no less than 72 h. The dosage of regenerant was 4%, 8% and 12% (abbreviated as: RE-4, RE-8 and RE-12) of the asphalt content in the old material. The content of SBR latex was 3% in emulsified asphalt.

2.2.2. Testing Method

The moisture susceptibility of the CRMEs was evaluated by the water immersion splitting tests and the split strength tests after freezing and thawing, and the high-temperature stability was evaluated by the rutting tests following the JTG/E20-2011 procedure [30]. The low-temperature crack resistance of CRMEs was evaluated by semi-circle bending (SCB) tests [31,32]. The height of the SCB test specimen was 25 mm, the diameter was 100 mm, the distance between two supports was 80 mm, and the test temperature was $-10\text{ }^{\circ}\text{C}$. A UTM-25 was applied for loading at a rate of 5 mm/min (shown in Figure 2). The tensile stress can be calculated according to Equation (1) [32]:

$$\sigma_t = \frac{4.888F}{DB} \quad (1)$$

where σ_t represents the tensile stress (MPa) at the bottom of the specimen; B represents the thickness (mm) of the specimen; D represents the diameter (mm) of the specimen; and F represents the vertical load (N). The tensile strain at the bottom of the specimen can be calculated by Equation (2).

$$\xi = \frac{6sD}{1.14D^2(5.578\frac{s}{D} - 1.3697)} = \frac{1.36d}{D} \quad (2)$$

where ξ represents the strain at the bottom center of the specimen; d represents the deflection (mm) at the center of the bottom of the specimen; and s represents the distance (mm) between two supporting rollers. The fracture energy density is defined in Equation (3).

$$\frac{dw}{dv} = \int_0^{\xi_0} \sigma d\xi \quad (3)$$

where $\frac{dw}{dv}$ represents the fracture energy density (KPa) and ξ_0 represents the strain value corresponding to the stress peak point in the stress–strain curve.



Figure 2. Instrument and specimen for semicircular bending test and dynamic modulus test.

The dynamic mechanical properties of the CRMEs were evaluated by uniaxial compression dynamic modulus tests following the JTG/E20-2011 procedure [30]. The superpave gyratory compactor (SGC) method was used to mold the specimen (diameter 100 mm, height 150 mm) (shown in Figure 2). Each group had 4 parallel specimens. The porosity of

specimen was $10\% \pm 1\%$. The temperature of the uniaxial compression dynamic modulus tests was $-10\text{ }^{\circ}\text{C}$, $0\text{ }^{\circ}\text{C}$, $10\text{ }^{\circ}\text{C}$, $15\text{ }^{\circ}\text{C}$ and $20\text{ }^{\circ}\text{C}$ and the loading waveform was sine wave. The load amplitude at each temperature is shown in Table 2. The dynamic modulus and phase angle were measured at 0.1 Hz, 0.5 Hz, 1 Hz, 5 Hz, 10 Hz, and 25 Hz at each temperature. Before the test, the specimen was pretreated by sine wave compressive stress test load with frequency of 25 Hz and 200 cycles.

Table 2. Load amplitude of dynamic modulus test.

Test temperature	$-10\text{ }^{\circ}\text{C}$	$0\text{ }^{\circ}\text{C}$	$10\text{ }^{\circ}\text{C}$	$15\text{ }^{\circ}\text{C}$	$20\text{ }^{\circ}\text{C}$
Load amplitude/kPa	2100	1400	700	700	400

The indirect tensile test was used to evaluate the fatigue resistance of the CRMEs. The test was performed in stress control mode, the test temperature was $15\text{ }^{\circ}\text{C}$, the loading frequency was 10 Hz, and the loading waveform was a half-sine wave. A large number of studies [33] have shown that the log fatigue life of the specimen under the same stress level is normally distributed, and the fatigue life and stress have a linear relationship on the double logarithmic coordinate. The fatigue life–stress relationship of the CRMEs can be expressed by the classic fatigue equation, as shown in the following Equation (4):

$$N = k(1/\sigma)^n \quad (4)$$

To fit the stress level and the fatigue life with double logarithmic coordinates, the equation is manipulated as shown in Equation (5):

$$\lg(N) = k - n \cdot \lg(\sigma) \quad (5)$$

where $\lg(N)$ represents the logarithm of fatigue life, σ represents the maximum loading stress, k represents the y-intercept of the line and n represents the slope of the line [33].

2.2.3. Efficacy Coefficient Method

The efficacy coefficient method is a quantitative evaluation method for the comprehensive analysis of multiple indicators. It is mainly used to evaluate the comprehensive benefits of a project. The process of this method is to determine a satisfactory value and a disallowed value for each evaluation index according to the conditions of the index. Taking the satisfactory value as the upper limit and the disallowed value as the lower limit to calculate the distance of each index from achieving the satisfactory value, and use this to determine the score of each indicator. Finally, each index score is weighted to obtain a comprehensive score, which is the total efficacy coefficient [34]. The specific processes are as follows:

(1) Determination of the evaluation index system

In determining the requirements for the evaluation index system of the efficacy coefficient method, the selected indicators should be representative, complement each other without repeating each other, and reflect the overall situation of the evaluation object as much as possible.

(2) Determination of the satisfactory value and disallowed value of each index.

The satisfactory value is the best limit value that each index data can reach, and the disallowed value is the worst limit value that each index data can reach.

(3) Calculation of the individual efficacy coefficient value of each index.

There are three variables in the evaluation system of the efficacy coefficient method. The highest value in the actual data and the highest individual efficacy coefficient are the maximal variables; the lowest the actual data and the highest the individual efficacy coefficient value are the minimal variables; and when the actual indicator data are at a certain value, the individual efficacy coefficient reaches the maximum, which is the stability variable.

The equations for the individual efficacy coefficients of the above three kinds of variables are as follows:

(1) Maximal individual efficacy coefficient:

$$d_{1i} = \begin{cases} \frac{X_i - X_{si}}{X_{hi} - X_{si}} \times 0.4 + 0.6 & X_i < X_{hi} \\ 1 & X_i \geq X_{hi} \end{cases} \quad (6)$$

(2) Minimal individual efficacy coefficient:

$$d_{2i} = \begin{cases} \frac{X_i - X_{si}}{X_{hi} - X_{si}} \times 0.4 + 0.6 & X_i > X_{hi} \\ 1 & X_i \leq X_{hi} \end{cases} \quad (7)$$

(3) Stability individual efficacy coefficient:

$$d_{3i} = (1 - |X_i - X_{hi}| / |X_{si} - X_{hi}|) \times 0.4 + 0.6 \quad (8)$$

where d_{1i} represents the individual efficacy coefficient of the i th maximal evaluation index; d_{2i} represents the individual efficacy coefficient of the i th minimal evaluation index; d_{3i} represents the individual efficacy coefficient of the i th stability evaluation index; X_i represents the actual value of the i th evaluation index; X_{hi} represents the satisfaction value of the i th evaluation index; X_{si} represents the disallowed value of the i th evaluation index.

(4) Determination of the weight of each indicator

According to the importance of each index, the analytic hierarchy process (AHP) is used to assign weight to each index.

First, according to the priority and importance of each index, the judgment matrix is established. Through the calculation rules of the AHP method, the weights of various indicators can be obtained by Equation (9):

$$w_i = \frac{1}{n} \sum_{j=1}^n \frac{a_{ij}}{\sum_{k=1}^n a_{kj}}, \quad (i = 1, 2, \dots, n) \quad (9)$$

where w_i represents the weight of each index, a_{ij} represents the elements of the i th row and j th column in the judgment matrix and a_{kj} represents the elements of the k th row and j th column in the judgment matrix.

After obtaining the weight of each index, Equations (10) and (11) are used to test the consistency of the matrix:

$$CI = \frac{\lambda_{\max} - n}{n - 1} \quad (10)$$

where CI represents the consistency index, λ_{\max} represents the maximum eigenvalue of the matrix, and n represents the order of the matrix.

$$CR = \frac{CI}{RI} \quad (11)$$

where CR represents the random one-time index and RI represents the average random one-time index.

If $CR < 0.1$, the judgment matrix passes the consistency test.

(5) Calculation of total efficacy coefficient

The total efficacy coefficient is calculated according to Equation (12) to obtain the total efficacy coefficient of different schemes.

$$D_i = \prod_1^n d_i^{w_i} \quad (12)$$

where D_i represents the total efficacy coefficient and d_i represents the individual efficacy coefficient of the i th evaluation index.

3. Results and Discussion

3.1. Moisture Susceptibility

The moisture susceptibility test results of different CRMEs are shown in Figures 3 and 4.

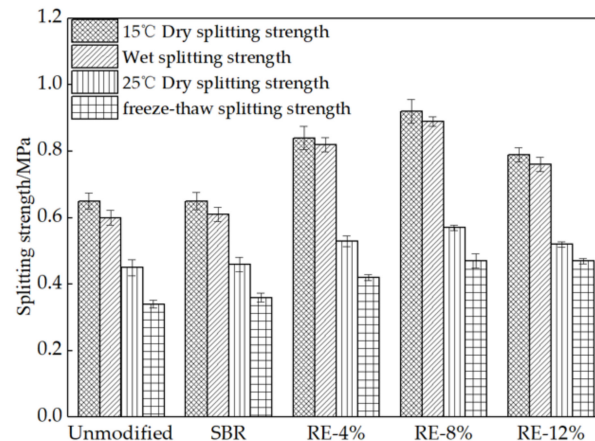


Figure 3. Dry-wet splitting strength and freeze-thaw splitting strength of the cold recycled mixture with asphalt emulsions (CRMEs).

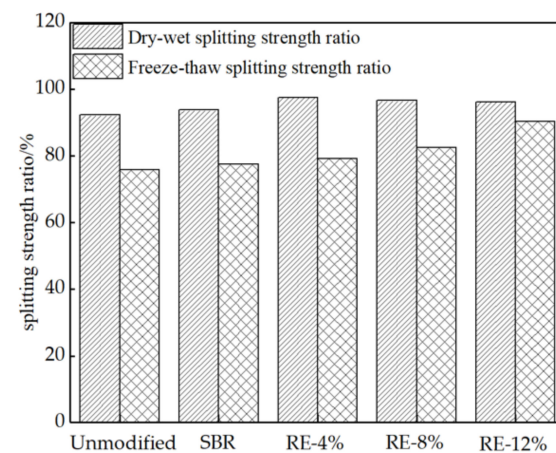


Figure 4. Residual splitting ratio of the CRMEs.

It can be seen from Figures 3 and 4 that when 4%, 8% and 12% of regenerant were added to the CRMEs, the dry splitting strength at 15 °C increased by 29%, 42% and 22%, respectively; the dry splitting strength at 25 °C increased by 18%, 27% and 16%, respectively; and the water immersion splitting strength at 15 °C increased by 37%, 48% and 27%, respectively. When SBR latex was used to modify the CRMEs, the increase in dry and wet splitting strength was not obvious. When adding 4%, 8%, and 12% of regenerant to the CRMEs, the freeze-thaw splitting strength increased by 23%, 38%, and 38%, respectively. However, when SBR latex was used to modify the CRMEs, the freeze-thaw splitting strength increased by 6%. The dry-wet splitting strength ratio and freeze-thaw splitting strength ratio of the CRMEs modified with regenerant and SBR latex were both improved, and both met the technical requirements of current specifications for asphalt surfaces. The reason for the improved strength may be that the regenerant can fuse with the old asphalt components, reduce the viscosity of the aged asphalt, improve the adhesion between the asphalt and the aggregate, and make the CRMEs easier to compact.

The micro-interfaces of the unmodified CRMEs and regenerant-modified CRMEs were tested by SEM [35,36], and the results are shown in Figures 5 and 6. The microscopic images show that the interface between the mortar and RAP aggregate in the regenerant-modified CRMEs is compactness and uniformity. After adding regenerant into the CRMEs, the regenerant forms a composite mortar system with the filler, cement and emulsified asphalt. The regenerant diffuses evenly into the CRMEs composite mortar system, infiltrating the aged asphalt in the RAP and improving the compactness of the composite mortar. In addition, by providing light oily components to the aged asphalt, the regenerant reduces the viscosity of the composite mortar, and the fluidity and workability of the mixture are increased, making the mixture denser and easier to compact and effectively improving the adhesion of the composite mortar.

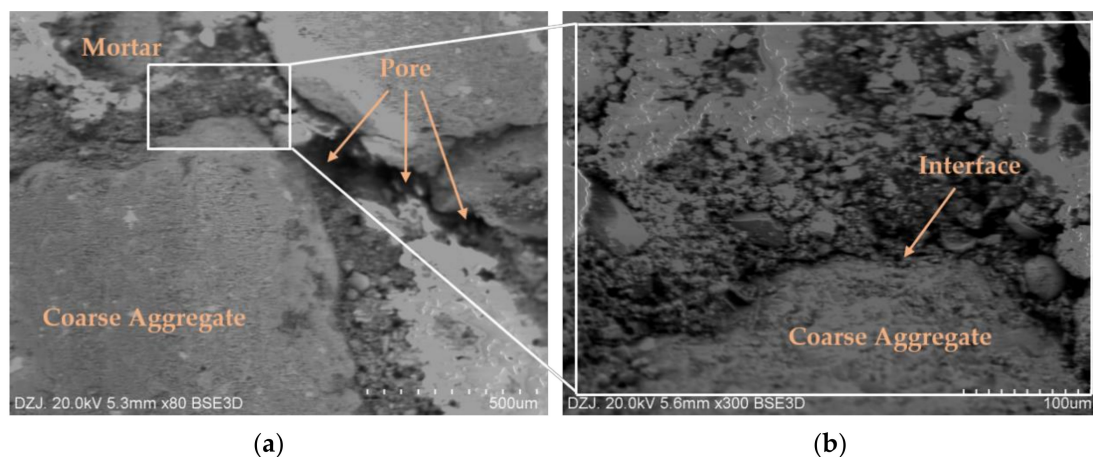


Figure 5. Microscopic image of the unmodified CRMEs: (a) image under 5.3mm \times 80 lens and (b) image under 5.6mm \times 300 lens.

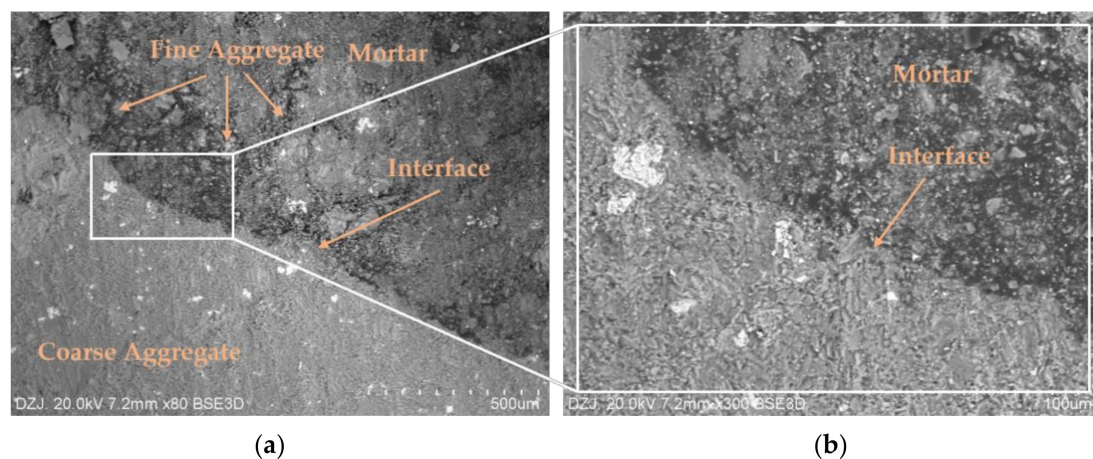


Figure 6. Microscopic image of the regenerant-modified CRMEs: (a) image under 7.2mm \times 80 lens and (b) image under 7.2mm \times 300 lens.

3.2. Crack Resistance at Low Temperature

The results of the SCB test are shown in Figure 7.

It can be seen from Figure 7 that when SBR latex was used to modify emulsified asphalt, the bending stress of the CRMEs increased by 21%. When 4%, 8% and 12% of regenerant were added, the bending stress of the CRMEs increased by 128%, 204% and 175%, respectively. With increasing regenerant content, the fracture energy density of the CRMEs also increased. When the regenerant content was 4%, 8%, and 12%, the fracture energy density increased by 120%, 189%, and 248%, respectively. However, the fracture energy density of SBR latex-modified CRMEs only increased by 8%, indicating that the

regenerant more obviously improved the crack resistance of the CRMEs at low-temperature. Because the mixture of regenerant and RAP could improve the compatibility, part of the aging asphalt was softened to improve the low-temperature tensile properties of the CRMEs.

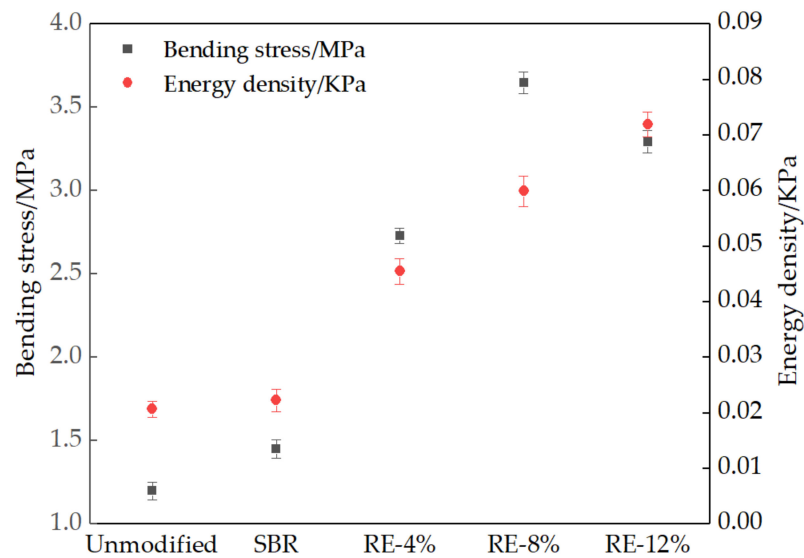


Figure 7. Results of the semi-circle bending (SCB) test.

3.3. High-Temperature Stability

The rutting test results of different types of CRMEs are shown in Figure 8.

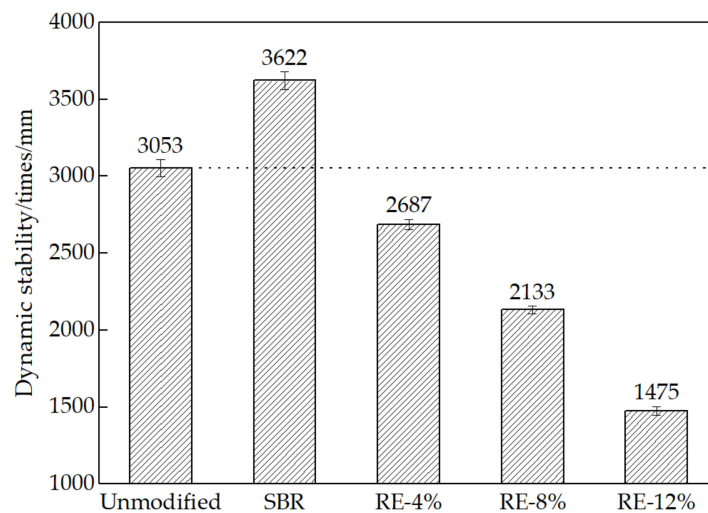


Figure 8. Dynamic stability at 60 °C of different types of CRME.

It can be seen from Figure 8 that the dynamic stability at 60 °C of the CRMEs made with SBR latex-modified emulsified asphalt increased by 19%, compared with dynamic stability of the unmodified CRMEs. When 4%, 8% and 12% of regenerant were added, the dynamic stability of the CRMEs decreased by 12%, 30% and 52%, respectively, and adding more regenerant resulted in a more obvious impact on the dynamic stability. Because the asphalt in the RAP becomes hard due to long-term aging, when the regenerant infiltrates into the RAP, it fuses with the chemical components of the aging asphalt, improving the rheological properties of the asphalt and making the aging asphalt soften noticeably. The greater the regenerant content is, the more obvious the softening of aging asphalt.

3.4. Analysis of Dynamic Response Parameters

3.4.1. Effect of Regenerant

The results of the dynamic modulus test for different CRMEs at a 10 Hz loading frequency are shown in Table 3. Dividing the dynamic modulus of different modified CRMEs by the dynamic modulus of unmodified CRMEs at the same temperature, the ratio is shown in Table 4.

Table 3. Dynamic modulus test results of different CRMEs at 10 Hz loading frequency.

Mixture Type	Dynamic Modulus/MPa					Phase Angle/°				
	−10 °C	0 °C	10 °C	15 °C	20 °C	−10 °C	0 °C	10 °C	15 °C	20 °C
Unmodified	7826	6272	4220	3786	2692	4.06	4.47	9.66	11.41	13.73
SBR	6078	4281	3433	3357	2321	4.66	6.07	8.92	10.67	13.08
RE-4%	9130	7284	5213	4444	3194	4.77	10.54	11.88	12.28	15.11
RE-8%	9998	7606	5236	4598	3276	5.90	7.05	10.87	12.24	16.01
RE-12%	5586	4336	2842	2432	/	8.17	11.07	15.7	16.48	/

Table 4. Ratio of dynamic modulus of the modified CRMEs and unmodified CRMEs.

Mixture Type	Ratio of Dynamic Modulus					Ratio of Phase Angle				
	−10 °C	0 °C	10 °C	15 °C	20 °C	−10 °C	0 °C	10 °C	15 °C	20 °C
SBR	0.78	0.68	0.81	0.89	0.86	1.15	1.36	0.92	0.94	0.95
RE-4%	1.17	1.16	1.24	1.17	1.19	1.17	2.36	1.23	1.08	1.10
RE-8%	1.28	1.21	1.24	1.21	1.22	1.45	1.58	1.13	1.07	1.17
RE-12%	0.71	0.69	0.67	0.64	/	2.01	2.48	1.63	1.44	/

Tables 3 and 4 show that the dynamic modulus of the SBR latex-modified CRMEs is less than unmodified CRMEs at any temperature. The phase angle of the SBR latex-modified CRMEs is larger than unmodified CRMEs at low temperature and finally less than unmodified CRMEs with increasing temperature. At the same temperature, the dynamic modulus of the CRMEs first increases and then decreases with increasing regenerant content. When the regenerant content was 4% and 8%, the dynamic modulus of the CRMEs were greater than unmodified CRMEs, and when the content of regenerant was 12%, the dynamic modulus was less than that of unmodified CRME. The phase angle of the CRMEs modified by regenerant was larger than unmodified CRMEs at any other temperature, which indicated that the addition of the regenerant can improve the viscosity of the CRMEs. There are limits to recovering the performance of aging asphalt when too little regenerant is used, but too much regenerant increased the fluidity of the mixture and reduces the strength of the CRMEs.

3.4.2. Master Curve of Dynamic Modulus

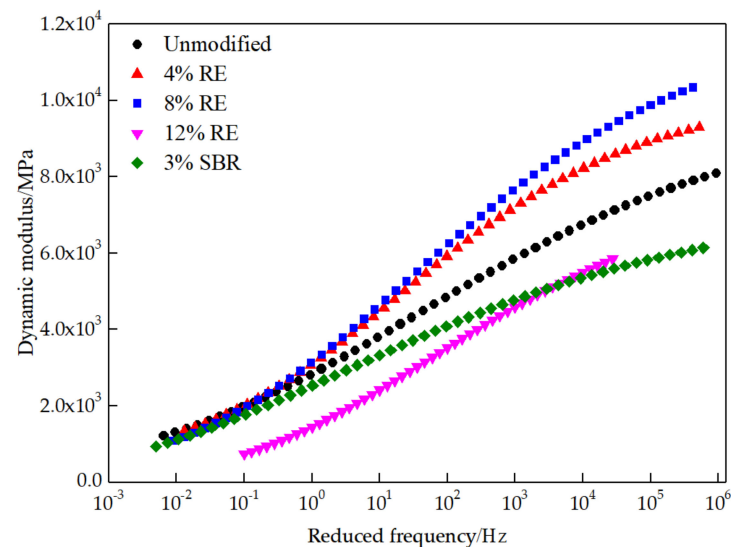
According to the principle of time-temperature equivalence (which means that the influence of loading time and environmental temperature on the mechanical behavior of asphalt binder is equivalent), a sigmoidal function [37] (shown in Equation (13)) was used to fit the dynamic modulus at different temperatures. The time-temperature conversion factors (which means the horizontal distance of different temperatures moving to the reference temperature) at different temperatures were obtained, as shown in Table 5, to translate the dynamic modulus image at different temperatures to form a master curve. The master curves of the dynamic modulus at 15 °C are shown in Figure 9.

$$\lg|E^*| = \delta + \frac{\alpha}{1 + \exp(\beta + \gamma \lg f_r)} \quad (13)$$

where E^* represents the complex modulus, δ represents the minimum asymptotic value, α represents the difference between minimum and maximum asymptotes, β and γ represents the shape parameter of the master curve.

Table 5. Calculation results of the time-temperature shift factor for different CRMEs.

Mixture Type	Time-Temperature Shift Factor				
	−10 °C	0 °C	10 °C	15 °C	20 °C
Unmodified	4.6532	2.4624	0.4771	0	−1.1871
SBR	4.4624	1.4771	0.0212	0	−1.3010
RE-4%	4.3979	2.0414	0.5563	0	−0.8861
RE-8%	4.3118	2.0000	0.3979	0	−1.0458
RE-12%	3.0969	1.7404	0.3617	0	/

**Figure 9.** Master curves of the dynamic modulus of different CRMEs.

It can be seen from Table 5 that the absolute value of the dynamic modulus curve shift factor of CRMEs modified by regenerant and SBR latex is less than that of unmodified CRMEs, indicating that its temperature sensitivity is weaker than that of unmodified CRMEs.

Analysis of Figure 9 shows that the master curve of the dynamic modulus of different CRMEs decreases with decreasing frequency (increasing temperature) because under high temperature or long-term loading, the asphalt softens, the internal friction resistance of the aggregate is reduced, and the deformation resistance of the mixture is also reduced. In the case of a low loading frequency (higher temperature), the master curves of other CRMEs tend to be the same except for CRMEs with a 12% regenerant content. In the case of a higher loading frequency (lower temperature), the order of the dynamic modulus values of the master curve of the five types of CRME from top to bottom is as follows: 8% regenerant > 4% regenerant > unmodified > SBR latex > 12% regenerant, which is consistent with the above conclusion about the dynamic modulus, that is, an appropriate content of regenerant can improve the dynamic modulus of the CRMEs, and when the content of regenerant is 8%, the dynamic modulus of the CRMEs reaches the maximum.

3.5. Fatigue Resistance

The indirect tensile fatigue test data of five CRME groups are plotted in Figure 10. The fatigue equations and relevant coefficients are shown in Table 6.

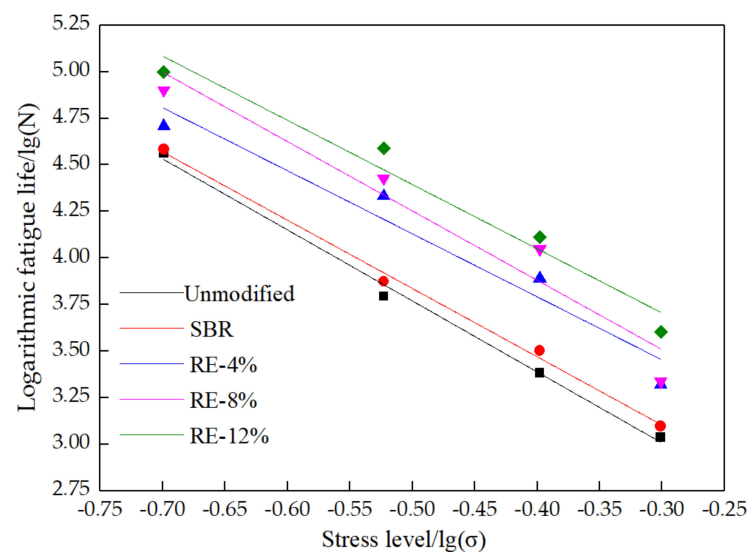


Figure 10. Fitting lines of logarithmic fatigue life of different CRMEs.

Table 6. Parameters of the logarithmic fatigue life fitting lines of CRMEs.

Mixture Type	Logarithmic Fatigue Equation	k	n	R ²
Unmodified	$\lg(N) = 1.862 - 3.815\lg(\sigma)$	1.862	3.815	0.995
SBR	$\lg(N) = 2.001 - 3.669\lg(\sigma)$	2.001	3.669	0.996
RE-4%	$\lg(N) = 2.435 - 3.389\lg(\sigma)$	2.435	3.389	0.949
RE-8%	$\lg(N) = 2.391 - 3.723\lg(\sigma)$	2.391	3.723	0.940
RE-12%	$\lg(N) = 2.670 - 3.449\lg(\sigma)$	2.670	3.449	0.968

Figure 10 and Table 6 show that the fatigue life of the unmodified and modified CRMEs decreases with loading stress increasing. The fatigue life of the CRMEs modified by regenerant and SBR latex are both higher than that of the unmodified CRMEs in low-stress areas and high-stress areas. Adding regenerant results in more significant improvement in the fatigue performance of the CRMEs than the SBR latex. The *n* value of the fatigue curve of the CRMEs modified with the regenerant and SBR latex decreased and the *K* value increased, indicating that the stress sensitivity of the CRMEs that was modified with the regenerant and SBR latex decreased and the fatigue resistance increased. Using a greater content of the regenerant resulted in a more obvious improvement in the fatigue resistance of the CRMEs.

3.6. Comprehensive Performance Evaluation

3.6.1. Evaluation Index System

Efforts were made to ensure that the selected indicators are representative and comprehensively reflect the overall evaluation. Different CRMEs freeze-thaw splitting tensile strength ratios (TSR), fracture energy densities (FED), dynamic stabilities (DS), dynamic moduli (DM), and parameters *k* and *n* in the fatigue fitting equation's six indexes were used to construct a comprehensive performance evaluation system (shown in Table 7).

Table 7. Technical performance indicators of different CRMEs.

Mixture Type	TSR/%	FED/KPa	DS/Times/mm	DM/MPa	k	n
Unmodified	75.8	0.0207	3053	3786	1.862	3.815
SBR	77.5	0.0223	3622	3357	2.001	3.669
RE-4%	79.2	0.0455	2687	4444	2.435	3.389
RE-8%	82.5	0.0599	2133	4598	2.391	3.723
RE-12%	90.4	0.0719	1475	2432	2.670	3.449

3.6.2. Individual Efficacy Coefficient

The indexes involved in this analysis are maximal variables except the parameter n in the fatigue fitting equation, which is a minimal variable. According to Equations (6) and (7), the individual efficiency coefficient of each index of different CRMEs is calculated as shown in Table 8.

Table 8. Individual efficiency coefficient of each evaluation index of different CRMEs.

Mixture Type	TSR/%	FED/KPa	DS/Times/mm	DM/MPa	k	n
Unmodified	0.6	0.6	0.8940	0.8500	0.6	0.6
SBR	0.6466	0.6125	1	0.7708	0.6688	0.7371
RE-4%	0.6932	0.7938	0.8258	0.9715	0.8837	1
RE-8%	0.7836	0.9063	0.7226	1	0.8619	0.6864
RE-12%	1	1	0.6	0.6	1	0.9437

3.6.3. Calculation of Weight Value

In this paper, the AHP judgment matrix (shown in Table 9) is determined based on the experience of many highway researchers, designers, construction personnel, management personnel and maintenance personnel. They all have intermediate or senior professional titles, extensive experience, and familiarity with expertise and management of asphalt pavement, so they are fully representative, and the evaluation results have high credibility.

Table 9. Table of analytic hierarchy process (AHP) judgment matrix.

Index	TSR	FED	DS	DM	k	n
TSR	1	4/3	1.5	1	8/3	8/3
FED	3/4	1	9/8	3/4	2	2
DS	2/3	8/9	1	2/3	16/9	16/9
DM	1	4/3	3/2	1	8/3	8/3
k	3/8	1/2	9/16	3/8	1	1
n	3/8	1/2	9/16	3/8	1	1

Substituting the data in the AHP judgment matrix into Equation (9) yields the weight of each index:

$$w_1 = \frac{1}{6} \sum_{j=1}^n \frac{a_{1j}}{\sum_{k=1}^n a_{kj}} = \frac{1}{6} (0.24 + 0.24 + 0.24 + 0.24 + 0.24 + 0.24) = 0.24 \quad (14)$$

Through the same calculation process, the values of w are obtained as follows: $w_2 = 0.18$, $w_3 = 0.16$, $w_4 = 0.24$, $w_5 = 0.09$, and $w_6 = 0.09$.

Substituting the values from the AHP judgment matrix into Equations (10) and (11) confirms the consistency.

$$CI = \frac{\lambda_{\max} - n}{n - 1} = \frac{6 - 6}{6 - 1} = 0 \quad (15)$$

$$CR = \frac{CI}{RI} = \frac{0}{1.24} = 0 \quad (16)$$

$CR < 0.1$, the AHP judgment matrix passes the consistency test.

3.6.4. Calculation of Total Efficacy Coefficient

The total efficacy coefficients of the performance of different CRMEs were calculated according to Equation (12):

$$D_1 = \prod_{i=1}^n d_i^{w_i} = 0.6^{0.24} \times 0.6^{0.18} \times 0.894^{0.16} \times 0.850^{0.24} \times 0.6^{0.09} \times 0.6^{0.09} = 0.6953 \quad (17)$$

$$D_2 = \prod_{i=1}^n d_i^{w_i} = 0.6466^{0.24} \times 0.6125^{0.18} \times 1^{0.16} \times 0.7708^{0.24} \times 0.6688^{0.09} \times 0.7371^{0.09} = 0.7269 \quad (18)$$

Through the same calculation, the following values were obtained: $D_3 = 0.8368$, $D_4 = 0.8391$, $D_5 = 0.8109$.

Figure 11 shows that the order of comprehensive performance of different CRMEs is RE-8% > RE-4% > RE-12% > SBR > unmodified. The results show that the comprehensive performance of CRMEs modified by the regenerant were better than that with the SBR latex, and the comprehensive performance of the CRMEs modified with 8% regenerant was the best.

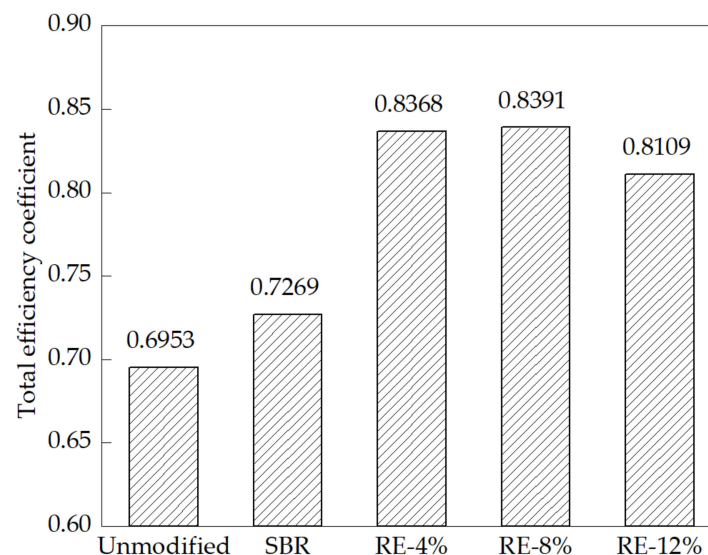


Figure 11. Total efficacy coefficient of different CRMEs.

4. Conclusions

(1) The addition of regenerant can significantly improve the crack resistance at low temperature and the moisture susceptibility of the CRMEs, while SBR latex has not been found to significantly improve the moisture susceptibility and low-temperature crack resistance of CRMEs. The addition of regenerant has a negative impact on the high-temperature performance of CRMEs, and the more regenerant that is used, the worse the high-temperature performance of the CRMEs, while SBR latex can improve the high-temperature performance of the CRMEs.

(2) The master curve of the dynamic modulus of the CRMEs increases gradually in an “s” shape with loading frequency increasing. A proper regenerant content can significantly increase the dynamic modulus of the CRMEs and reduce its temperature sensitivity. The fatigue life of the CRMEs modified with the regenerant and SBR latex is much higher than that of unmodified CRMEs at both low stress and high stress conditions. The improvement in the anti-fatigue performance of the regenerant-modified CRMEs is significant. The greater the content of the regenerant, the more obvious the improvement for the anti-fatigue performance of the CRMEs.

(3) The regenerant can form a composite mortar system with filler, cement and emulsified asphalt such that the interface between the mortar and RAP aggregate has more compactness and uniformity, improving the cohesion of the mixture.

(4) Adding regenerant can significantly improve the moisture susceptibility, low-temperature crack resistance, fatigue resistance and dynamic modulus of CRMEs, but a higher regenerant content does not necessarily create better performance. The order of comprehensive performance of different CRMEs is RE-8% > RE-12% > RE-4% > SBR > unmodified, and the optimal regenerant content is 8%.

Author Contributions: D.W. and T.G. conceived and designed the research; D.W. drafted the manuscript and prepared figures; T.G. and H.C. drafted, reviewed, and edited the manuscript; Y.C., X.Y. and T.W. discussed the results. All authors have read and agreed to the published version of the manuscript.

Funding: This research was funded by The National Key Technologies R&D Program of China(2018YFE0120200), North China University of Water Resources and Electric Power High-level Talent Research Start-up Project(202009005) and Open Fund Project of Henan Province Engineering Technology Research Center for Environment-friendly and High-performance Pavement Materials (Henan Science foundation [2020] No.18).

Institutional Review Board Statement: Not applicable.

Informed Consent Statement: Not applicable.

Data Availability Statement: Not applicable.

Conflicts of Interest: The authors declare no conflict of interest.

References

- Li, H.X. *Research on Asphalt Cold Recycled Mixture Performance and Pavement Structure*; Beijing Jiaotong University: Beijing, China, 2018.
- Li, F.; Yan, J.H.; Han, P. Evaluation of Early Strength of Emulsified Asphalt Cold Recycled Mixture. *J. China Foreign Highw.* **2016**, *36*, 273–275.
- Martina, I.G.; Giovanni, D.; Nicolò, B. Comparative life cycle assessment of asphalt pavements using reclaimed asphalt, warm mix technology and cold in-place recycling. *Resour. Conserv. Recycl.* **2015**, *104*, 224–238.
- Gu, F.; Yan, J.H.; Han, P. Structural performance and sustainability assessment of cold central-plant and in-place recycled asphalt pavements: A case study. *J. Clean. Prod.* **2019**, *208*, 1513–1523. [[CrossRef](#)]
- Xiao, F.P.; Yao, S.L.; Wang, J.G. A literature review on cold recycling technology of asphalt pavement. *Constr. Build. Mater.* **2018**, *180*, 579–604. [[CrossRef](#)]
- Daryaei, D.; Ameri, M.; Mansourkhaki, A. Utilizing of waste polymer modified bitumen in combination with rejuvenator in high reclaimed asphalt pavement mixtures. *Constr. Build. Mater.* **2020**, *235*, 117516. [[CrossRef](#)]
- Ali, B.; Mahsa, M.G.; Farhad, G.A. Effects of copper slag and recycled concrete aggregate on the properties of CIR mixes with bitumen emulsion, rice husk ash, Portland cement and fly ash. *Constr. Build. Mater.* **2015**, *96*, 172–180.
- Ayar, P. Effects of additives on the mechanical performance in recycled mixtures with bitumen emulsion: An overview. *Constr. Build. Mater.* **2018**, *178*, 551–561. [[CrossRef](#)]
- Wang, Y.Y.; Zhen, L.; Xi, L. Cold recycling of reclaimed asphalt pavement towards improved engineering performance. *J. Clean. Prod.* **2018**, *17*, 1031–1038. [[CrossRef](#)]
- Mohsen, A.O.; Amir, M. Emulsified cold recycled mixture using cement kiln dust and coal waste ash-mechanical-environmental impacts. *J. Clean. Prod.* **2018**, *199*, 101–111.
- Jiang, J.; Ni, F.; Zheng, J. Improving the high-temperature performance of cold recycled mixture by polymer-modified asphalt emulsion. *Int. J. Pavement Eng.* **2020**, *21*, 41–48. [[CrossRef](#)]
- Yang, D.G. Effects of different fibers on the mechanical and road performance of emulsified asphalt cold recycled mixture. *Highway* **2020**, *3*, 1–7.
- Deng, C.Q.; Jiang, Y.J.; Lin, H.W. Influence of gradations on performance of emulsified asphalt cold recycled mixture produced using vertical vibration compaction method. *Road Mater. Pavement Des.* **2019**, *1*, 1–21. [[CrossRef](#)]
- Han, Q.K.; Li, X.M.; WEID, B. Effect of latex admixture on the low temperature performance of emulsified asphalt cold regeneration. *Bull. Chin. Ceram. Soc.* **2015**, *34*, 3197–3201.
- Li, Y.F. Study on durability of emulsion asphalt cold recycled mixture with different dosage of waterborne epoxy resin. *Highw. Eng.* **2016**, *41*, 82–87.
- Chen, C.; Xue, J.R. Study on strength characteristics and road performance of rubber powder modified emulsified asphalt cold reclaimed mixture. *Highw. Eng.* **2020**, *41*, 72–77.

17. Li, J.; Fu, W.; Yin, X. Proportion Design Method and Water Stability of Cement-Emulsified Asphalt Cold Recycling Mixture. *MATEC Web Conf.* **2018**, *238*, 05009. [[CrossRef](#)]
18. Yan, J.H.; Ni, F.J.; Yang, M.K. Indirect tensile fatigue performance of emulsified asphalt cold recycled mixture. *J. Build. Mater.* **2011**, *14*, 58–61.
19. Stimilli, A.; Ferrotti, G.; Graziani, A. Performance evaluation of a cold-recycled mixture containing high percentage of reclaimed asphalt. *Road Mater. Pavement Des.* **2013**, *14*, 13. [[CrossRef](#)]
20. Lyu, Z.; Ai Qin, S.; Xiao, Q. Grey target optimization and the mechanism of cold recycled asphalt mixture with comprehensive performance. *Constr. Build. Mater.* **2019**, *198*, 269–277. [[CrossRef](#)]
21. Zhang, J.L.; Zheng, M.L.; Pei, J.Z. Research on Low Temperature Performance of Emulsified Asphalt Cold Recycled Mixture and Improvement Measures Based on Fracture Energy. *Materials* **2020**, *13*, 3176. [[CrossRef](#)] [[PubMed](#)]
22. Pi, Y.H.; Li, Y.; Pi, Y.X. Strength and Micro-Mechanism Analysis of Cement-Emulsified Asphalt Cold Recycled Mixture. *Materials* **2019**, *13*, 128. [[CrossRef](#)]
23. Li, Z.G.; Hao, P.W.; Xu, J.Z. The effect of freeze-thaw cycles on the shear resistance of emulsified asphalt cold recycled mixture. *Mater. Rev.* **2016**, *30*, 121–125.
24. Wei, T.Z.; Hong, J.X.; Lin, J.T. Effect and mechanism of cement and emulsified asphalt on cold recycling strength. *J. Build. Mater.* **2017**, *20*, 310–315.
25. Liu, L. *Surface Characteristics and Performance Improvement of RAP*; Chang'an University: Xi'an, China, 2016.
26. Li, Z.G.; Wang, D.C.; Li, L.J. Effect of filler content on macro and micro properties of cold recycled emulsified asphalt mixture. *Highway* **2020**, *65*, 27–32.
27. Yang, Y.H.; Wu, Y.H.; Yang, Y. Macro and micro analysis of the influence of cement on the performance of emulsified asphalt cold recycling material. *Highw. Transp. Technol.* **2018**, *35*, 1–8.
28. MOC of PRC. *Technical Specifications for Construction of Highway Asphalt Pavements (JTG F40-2004)*; Ministry of Communications of the People's Republic of China: Beijing, China, 2004.
29. MOC of PRC. *Technical Specifications for Highway Asphalt Pavement Recycling (JTG/T5521-2019)*; Ministry of Communications of the People's Republic of China: Beijing, China, 2019.
30. MOC of PRC. *Standard Test Methods of Bitumen and Bituminous Mixtures for Highway Engineering (JTG E20-2011)*; Ministry of Communications of the People's Republic of China: Beijing, China, 2011.
31. Chen, X.H.; Li, W.N.; Li, H.T. Evaluation of fracture properties of epoxy asphalt mixture by SCB test. *J. Southeast Univ.* **2009**, *25*, 527–530.
32. Bayomy, F.; Mullaglanm, A.; Abdo, A.A. Evaluation of hot mix asphalt (HMA) fracture resistance using the critical strain energy release rate. *Transp. Res. Board Meeting* **2006**.
33. Wang, D.C.; Hao, P.W.; Wei, X.L. Fatigue performance and influence factor for cold recycling mixture with emulsified asphalt. *J. Beijing Univ. Technol.* **2016**, *42*, 541–546.
34. Jiang, J. Application of efficiency coefficient method in early warning of financial risks in colleges and universities. *Account. Financ.* **2009**, *5*, 56–60.
35. Wang, C.; Chen, Q.; Guo, T.; Li, Q. Environmental effects and enhancement mechanism of graphene/tourmaline composites. *J. Clean. Prod.* **2020**, *262*, 121313. [[CrossRef](#)]
36. Liu, K.; Fu, C.L.; Xu, P.X.; Li, S.Q.; Huang, M.Y. An eco-friendliness inductive asphalt mixture comprising waste steel shavings and waste ferrites. *J. Clean. Prod.* **2021**, *283*, 124639. [[CrossRef](#)]
37. Luo, R.; Xu, Y.; Liu, H.Q. Rheological properties of DCLR modified asphalt. *Chin. J. Highw.* **2018**, *31*, 165–171.